

11-70
57124
p24

**NASA
Technical
Memorandum**

NASA TM -103557

**HIGH-FREQUENCY DATA OBSERVATIONS FROM
SPACE SHUTTLE MAIN ENGINE LOW PRESSURE
FUEL TURBOPUMP DISCHARGE DUCT FLEX JOINT
TRIPOD FAILURE INVESTIGATION**

By T.F. Zoladz and R.A. Farr

Structures and Dynamics Laboratory
Science and Engineering Directorate

December 1991

(NASA-TM-103557) HIGH-FREQUENCY DATA
OBSERVATIONS FROM SPACE SHUTTLE MAIN ENGINE
LOW PRESSURE FUEL TURBOPUMP DISCHARGE DUCT
FLEX JOINT TRIPOD FAILURE INVESTIGATION
(NASA) 24 p

N92-13279

Unclas
0057124

CSCL 21H 63/20



National Aeronautics and
Space Administration

George C. Marshall Space Flight Center

REPORT DOCUMENTATION PAGE

Form Approved
OMB No. 0704-0188

Public reporting burden for this collection of information is estimated to average 1 hour per response, including the time for reviewing instructions, searching existing data sources, gathering and maintaining the data needed, and completing and reviewing the collection of information. Send comments regarding this burden estimate or any other aspect of this collection of information, including suggestions for reducing this burden, to Washington Headquarters Services, Directorate for Information Operations and Reports, 1215 Jefferson Davis Highway, Suite 1204, Arlington, VA 22202-4302, and to the Office of Management and Budget, Paperwork Reduction Project (0704-0188), Washington, DC 20503.

1. AGENCY USE ONLY (Leave blank)		2. REPORT DATE December 1991	3. REPORT TYPE AND DATES COVERED Technical Memorandum	
4. TITLE AND SUBTITLE High-Frequency Data Observations From Space Shuttle Main Engine Low Pressure Fuel Turbopump Discharge Duct Flex Joint Tripod Failure Investigation			5. FUNDING NUMBERS	
6. AUTHOR(S) T.F. Zoladz and R.A. Farr				
7. PERFORMING ORGANIZATION NAME(S) AND ADDRESS(ES) George C. Marshall Space Flight Center Marshall Space Flight Center, Alabama 35812			8. PERFORMING ORGANIZATION REPORT NUMBER	
9. SPONSORING / MONITORING AGENCY NAME(S) AND ADDRESS(ES) National Aeronautics and Space Administration Washington, DC 20546			10. SPONSORING / MONITORING AGENCY REPORT NUMBER NASA TM-103557	
11. SUPPLEMENTARY NOTES Prepared by Component Assessment Branch and Induced Environments Branch, Structures and Dynamics Laboratory, Science and Engineering Directorate.				
12a. DISTRIBUTION / AVAILABILITY STATEMENT Unclassified-Unlimited			12b. DISTRIBUTION CODE	
13. ABSTRACT (Maximum 200 words) This report summarizes observations made by MSFC Structures and Dynamics Laboratory engineers during their participation in the space shuttle main engine (SSME) low pressure fuel turbopump discharge duct flex joint tripod failure investigation. New signal processing techniques used by the Component Assessment Branch and the Induced Environments Branch during the failure investigation are described in detail. Moreover, nonlinear correlations between frequently encountered anomalous frequencies found in SSME dynamic data are discussed. Finally, the report concludes by recommending the continuation of low pressure fuel (LPF) duct testing through laboratory flow simulations and MSFC-managed technology test bed (TTB) SSME testing.				
14. SUBJECT TERMS SSME, Flex Joint, High Frequency			15. NUMBER OF PAGES 24	
			16. PRICE CODE NTIS	
17. SECURITY CLASSIFICATION OF REPORT Unclassified	18. SECURITY CLASSIFICATION OF THIS PAGE Unclassified	19. SECURITY CLASSIFICATION OF ABSTRACT Unclassified	20. LIMITATION OF ABSTRACT Unclassified	



TABLE OF CONTENTS

	Page
I. INTRODUCTION	1
II. OBSERVATIONS	2
A. "330 Hz"	2
B. High-Frequency Anomalous Activity	3
C. Similarities Between "12 kHz" and High-Frequency Anomalous Activity	6
III. CONCLUSIONS AND RECOMMENDATIONS	6
REFERENCES	8

LIST OF ILLUSTRATIONS

Figure	Title	Page
1.	Transducer location	9
2.	904-080 and 904-093 thrust profiles	10
3.	PSD's showing "330 Hz" activity, SSME static firing 904-093	11
4.	TOPO plots of LPF duct dynamic pressure for tests 904-080 and 904-093	12
5.	Experimental edgetone acoustics	13
6.	PSD's of LPF duct DY PR KFIFH and FJ "C" D-Z accel	14
7.	PDA coherence plots	15
8.	Bicoherence plot HPFTP inlet at KFIFH	16
9.	Corresponding PSD for bicoherence plot of figure 8	16
10.	TOPO of 904-072 HPFTP radial accel data	17
11.	TOPO of 904-093 HPFTP radial accel data	18
12.	TOPO of 904-093 HPFP high-frequency inlet pressure at KFIFH	19

TECHNICAL MEMORANDUM

HIGH-FREQUENCY DATA OBSERVATIONS FROM SPACE SHUTTLE MAIN ENGINE LOW PRESSURE FUEL TURBOPUMP DISCHARGE DUCT FLEX JOINT TRIPOD FAILURE INVESTIGATION

I. INTRODUCTION

Over the past year, the Component Assessment Branch (ED23) and the Induced Environments Branch (ED33) have been monitoring high-frequency accel, strain, and pressure data taken from instrumented low-pressure fuel (LPF) ducts in support of the space shuttle main engine (SSME) LPF duct flex joint (FJ) "C" tripod leg failure investigation. The Rocketdyne failure investigation final report¹ concludes that two flex joint failures were caused by increased loading of the LPF duct due to a pressure pulse at high-pressure fuel turbopump (HPFTP) synchronous speed. The report describes that this increased loading coupled with undersized radii in the flex joints was enough to cause the tripod leg failure. The Rocketdyne report also states that pressure pulse values measured on current engines are half of those experienced by the failed LPF ducts.

The Marshall Space Flight Center (MSFC) investigation has centered around the anomalous frequencies which have been routinely observed on the low pressure fuel turbopump (LPFTP) and the HPFTP along with newly observed frequencies being reported in LPF duct data. To date, the investigation has not been able to identify or verify any failure mechanisms associated with these frequencies which could have led to the FJ "C" tripod leg failure which occurred during hotfire 902-471 in June of 1989. However, several interesting observations regarding these high-frequency data have been made, and further investigation could provide insight into the flex joint failure investigation and anomalous phenomena commonly observed in SSME turbopump accel data.

Up to now, the "330 Hz" phenomena, seen in LPFTP data, and the "12 kHz" phenomena, common in HPFTP pump-end accel data, have been studied as two unrelated anomalies. However, review of the LPF duct data at high frequencies (>10 kHz) together with the utilization of new signal processing techniques developed for the Structures and Dynamics Laboratory at MSFC by Dr. Jen-Yi Jong of Wyle Laboratories²⁻⁵ have revealed a possible link between the two phenomena.

This report derives its observations from high-frequency (accel, strain, and pressure) data taken from various locations along the LPFTP-LPF duct-HPFTP fuel flow path during SSME static firings 904-080, 904-093, 904-094, and 904-095 (table 1). Along with pressure transducers at both LPFTP discharge and HPFTP inlet, various strain gauges and accels mounted on the LPF duct have revealed unique high-frequency activity. Figure 1 shows the general LPF duct transducer configuration for these four tests. While data from all four of the tests support our observations, this report emphasizes results from 904-093 and 904-080 since their slow power level sweep conditions ideally suited (fig. 2) the type of investigation performed with the high-frequency data.

Table 1. E0213 major component history.

<u>Component</u>	<u>904-080</u>	<u>904-093</u>	<u>904-094</u>	<u>904-095</u>
LPFTP U/N	2411R1	2411R1	2215	2411R1
HPFTP U/N	4306	4405	4013	6401
LPOTP U/N	2311	2222	2222	2222
HPOTP U/N	4304R1	4304R2	6009	4506
LPFD S/N	4918062	4911319	4911319	4911319

II. OBSERVATIONS

A. "330 Hz"

Standard posttest processing of LPFTP accel data from static firing 904-093 revealed "330 Hz" activity which included multiple modulation sidebands resulting from "330 Hz" combining with LPFTP synchronous and synchronous multiples. This activity is common in LPFTP data and is highly dependent on engine fuel inlet conditions. Several studies have been performed on "330 Hz" over the past 10 years⁶⁻⁸ which have identified key characteristics regarding the anomalous phenomena. Two anomalous frequencies are dominant in the analyses. These frequencies, labelled "2,700 Hz" and "1,300 Hz," do not appear in LPFTP data at the same time. They alternate (i.e., "swap out") with each other according to engine fuel inlet pressure. Amplitudes for "2,700 Hz" are much higher than the "1,300 Hz" component with maximum amplitudes as high as 120 Grms as seen in data from static firing 902-461.⁸ The "330 Hz" component is the lower 4N (four times LPFTP synchronous) sideband of "1,300 Hz" which in turn is ~50 percent of "2,700 Hz." Again, this anomalous frequency activity is highly dependent on LPFTP inlet conditions with the "2,700 Hz" component initiating at fuel inlet pressures below 20 psi and "330 Hz/1,300 Hz" initiating at ~9.5 psi. The "330 Hz" activity seen in 904-093 standard posttest data behaves consistently with characteristics listed in the references.

Interestingly, LPF duct high-frequency pressure, strain, and accel data also exhibited "330 Hz" activity. In fact, the anomaly could be clearly identified in high-frequency pressure data taken from pressure port KFIFH at HPFTP fuel inlet, joint F3 (fig. 1). Table 2 lists the amplitudes of the predominant "330 Hz" related frequencies seen in high frequency data from static firing 904-093 according to transducer type and location. The maximum amplitude for each spectral component was found using an anomalous frequency tracking filter over the duration of the 465-s test. The "2,700 Hz" frequency is not evident in the 904-093 data; however, the lower 4N sideband (1,820 Hz) is readily apparent. The multiple channel power spectral density (PSD's) plots of figure 3 show the spectral distribution of "330 Hz" activity over several transducers extending from the LPFTP to the HPFTP via the LPF duct. The "330-Hz" related components' peak amplitudes and spectral locations (table 2 and fig. 3) should be noted. Peak rms values taken from LPFTP discharge and HPFTP inlet range between 0.3 psi rms to 1.0 psi rms over the various "330 Hz" related frequencies seen in 904-093 high-frequency data. The presence of these frequencies was not addressed in the Rocketdyne report.¹ Our engineers feel that the presence of these pressure pulses should be addressed since they are of sufficient amplitude to warrant investigation into their roles as possible excitation sources of duct modes.

Table 2. “330 Hz” related frequency peak rms amplitudes during 904-093.

SENSOR	SPECTRAL COMPONENT			
	“330 Hz”	4N-2•“330 Hz”	2•“330 Hz”	4N-“330 Hz”
LPFP RAD 240 ACCEL(Grms)	2.3	0.6	0.9	0.8
LPFD DY PR JF2AH(psi rms)	0.9	1.0	0.8	0.5
FJ “C” D-Z ACCEL(Grms)	2.5	0.9	3.0	*
DY PR KFIFH(psi rms)	0.8	0.8	0.6	0.3
HPFP RAD 90 ACCEL(Grms)	*	*	*	*

*component not discrete enough to track

B. High-Frequency Anomalous Activity

One of the most interesting observations to come from this LPF duct investigation deals with the discovery of a multitude of anomalous frequencies in the 10 to 18 kHz spectrum. This anomalous behavior was not seen in LPFTP accel data, but it was observed in data taken from high-frequency transducers starting with LPFP high-frequency discharge pressure at F2 (JF2AH) through HPFTP radial accels (see fig. 1 for transducer location).

Figure 4 includes two TOPO plots showing frequency versus time history of the 10 to 18 kHz activity using high-frequency pressure data from HPFP inlet F3 (KFIFH). The TOPO plot, or topographic mapping of amplitude/frequency behavior versus time, is one of several new signal processing techniques being developed by Dr. Jong of Wyle Laboratories. The TOPO plot eliminates threshold-related problems which are common in the plotting of isoplots (waterfall plots) which also show amplitude/frequency versus time behavior for a signal. Typically, when threshold levels are too high, low amplitude components are severely depressed; however, too low a threshold will allow the noise floor to compress or confuse the isoplot. TOPO identifies the noise floor of a signal while stepping through time and then normalizes each PSD so that all spectral peaks are referenced to this noise floor. This eliminates threshold-related worries. TOPO does not enhance a spectrum by bringing out components lost in the noise floor as techniques such as adaptive filtering do; however, TOPO does maximize the utility of the PSD in the display of frequency versus time histories. Figure 4 shows that for tests 904-080 and 904-093, there are several peaks in the dynamic pressure data above 10 kHz which track differently than pump-related synchronous components. These frequencies appear to be centered around 11 kHz and 17 kHz, with the magnitude of the 17 kHz being generally higher than that of the 11 kHz. These anomalous frequencies are present in the data from all four tests described here, but their behavior is better defined in pressure data from test 904-080.

Upon examining figure 4, one will notice that these anomalous high frequencies do not occur at the same time, but seem to swap out similar to the “1,300 Hz” and “2,700 Hz” phenomena described in references 7 and 8, appearing and disappearing as a function of engine thrust and fuel flow velocity in the LPF duct. This behavior strongly implicates an acoustic/flow interaction as the source of both sets of anomalous frequencies. In addition, data from test 904-080 indicate the 11 to 17 kHz swap occurs at 88-percent rated power level (RPL) on the ramp up and at 85 percent on the ramp down. This hysteresis effect is another strong indicator of acoustic behavior. This effect is only quantifiable on slow ramps and should be verified with more tests.

Based on the above observations, a highly probable source of the 11 to 17 kHz and 1,300 to 2,700 Hz frequencies is that of a fuel flow velocity/shear layer impinging upon a sharp edge in the fuel side of the engine somewhere upstream of the HPFTP. Figures 5 and 6 describe experimentally determined characteristics of such edgetones. This phenomenon has been studied extensively and, once the source of the acoustic instability has been determined, is a fairly straightforward problem to correct.

Figures 5a and 5b, from the classic works of Brown and Wood,^{9 10} show the abrupt jumps in frequency characteristic of edgetones. Each jump to a higher frequency, or stage, is accompanied by an increase in amplitude of the acoustic energy. The path taken as flow increases is measurably different than that for decreasing flow velocity. The frequency of the edgetone is a function of fluid characteristics, such as pressure, temperature, density, fluid velocity, shear layer thickness, and sharpness of the impingement edge. Figure 5b illustrates the coupling that can occur between an edgetone and the duct, or organ pipe, in which it is located, with the duct modulating and stabilizing the frequency between jumps. These data suggest that the 10 to 18 kHz and 1,300 to 2,700 Hz phenomena originate in a shear layer-edge interaction which is being modulated and kept constant in frequency by acoustic characteristics of the LPF duct.

Figure 6 contains two PSD's showing amplitudes for the anomalous components at 104-percent RPL at both HPFP and FJ "C" D-Z accel locations from test 904-093. Taking the rms amplitude from the strongest anomalous component in the 10 to 18 kHz band of figure 6, a peak-to-peak estimation of displacement at the FJ "C" D-Z accel due to the spectral component can be made using the formula:

$$d_{p-p} = 703 \cdot Grms \cdot f^{-2}$$

where d_{p-p} : peak-to-peak amplitude in mm
 f : frequency of sinusoidal component
 $Grms$: rms estimation of component

Using this method, the rms estimation from the anomalous component at 16,450 Hz in figure 6 would predict a displacement of 1.66 (10^{-5}) mm at the FJ "C" D-Z accel (this estimation also includes correction for low pass filtering of the channel at 5 kHz). This very small displacement exhibits the spatial amplitude versus frequency relationship for very high spectral components. Since displacement is inversely proportional to the square of the frequency, a tremendous acceleration amplitude is required at high frequencies to produce a notable displacement. The above estimation assumes the anomalous component to be a perfect sinusoid. This assumption is shown to be somewhat reasonable through the use of phase domain averaging (PDA) techniques also developed by Dr. Jong. PDA defines the degree of discreteness of a spectral component by tracking the relative phase between the spectral component of interest and a reference sine wave at the same frequency. PDA increases the phase resolution of this component through chirp z-transform and then calculates the coherence of relative phase difference between the studied signal and the analytic sinusoid at the same frequency. This tool, as a means of determining discreteness of a signal, has several advantages over the more traditional method which utilizes probability density functions (PDF). The PDA method is much less sensitive to noise and to amplitude variation in the subject frequency than the PDF methods are. The PDA technique is sensitive however to variation in the frequency of the component of interest. This frequency variation results in phase distortion which then corrupts the PDA coherence.

Traditional PDF methods rely on the bandpass filtering of the subject time signal. This filtering, in addition to extending processing time, may distort the waveform of the filtered component. Unlike PDF, PDA does not rely on bandpass filtering. PDA operates on the ordinary time history and develops a relative coherence spectrum for a specified frequency band. This aspect of the method was essential in this LPF duct study due to the proximity in frequency of the spectral components in the 10 to 18 kHz band seen in figure 6. Traditional bandpass filtering could not be implemented with the LPF duct data since the subject anomalous frequencies could not be separated due to roll-off limitations of the digital filter. Figure 7 shows PDA coherence results for several spectral components found in the PSD's of figure 6. Figure 7a shows the relative coherence of both the LPFTP synchronous (N) and "330 Hz" components over three different transducers. Figures 7b and 7c show the PDA coherences for HPFTP synchronous multiples 12N' and 24N', respectively, over the same transducers. Finally, figures 7d and 7e show the PDA coherence results for the anomalous frequencies at 16,120 Hz and 16,450 Hz, respectively. Note how discrete the anomalous frequencies at 16,120 Hz and 16,450 Hz are as compared to the higher multiples of HPFTP synchronous of whose PDA coherences are shown in figures 7b and 7c (and that of LPFTP synchronous in figure 7a). 12N' and 24N' have very low PDA coherence since the frequency variation in synchronous is amplified by 12 and 24 times in the respective components. The high PDA coherences (a value of 1 represents perfect periodicity) for these anomalous components strongly support the contention that these anomalies are periodic in nature.

Another very interesting finding of this study deals with the relationship between "330 Hz" activity in the 1 kHz spectrum and the anomalous frequencies in the 10 to 18 kHz spectrum. Again, a new signal identification tool developed by Dr. Jong²⁻⁵ has proven its utility. In this case, the application of bicoherence to LPF duct data shows nonlinear interaction between "330 Hz" components and anomalous frequencies in the 10 to 18 kHz spectrum. Figure 8 is a bicoherence plot generated from high frequency pressure data taken from HPFTP fuel inlet, port KFIFH, during 104-percent RPL. In generating the bicoherence plot, three frequencies are involved. The first frequency, f1, is a constant frequency of interest, and, in this case, f1 is 305 Hz (the "330 Hz" anomalous frequency). The second argument, f2, is a sweep frequency which serves as the abscissa for the bicoherence plot. In figure 8, at a sweep frequency of 15,810 Hz, a bicoherence of 0.643 is identified. The peak indicates that some type of nonlinear interaction between f1, f2, and f1+f2 exists. The third frequency of interest, f3, is the sum frequency, f1+f2, in the bispectral analysis and is implicit in the estimation of the bicoherence. Therefore, f3 is not shown in the bicoherence plot. In this example, the sum frequency is 16,120 Hz. Figure 9 is a PSD showing the respective amplitudes of the three components. The "330-Hz" component at 305 Hz is plainly visible at low end of the spectrum while f2 just barely pierces the noise floor at 15,810 Hz. The sum frequency at 16,120 Hz has the highest amplitude of all the anomalous components in the 10 to 18 kHz band as shown in figure 9. The coherence value of 0.643 ($B_{xxx,a-p}(305,15810,16120) = 0.643$) indicates that at least 64.3 percent of the energy in the sum frequency at 16,120 Hz can be correlated to the component frequencies at 305 and 15,810 Hz. The other uncorrelated 35.7 percent could be due to noise corruption of the three components.

Trispectral analysis, similar to bispectra but taken to the next order, indicates similar levels of interaction amongst the anomalous frequencies in the 10 to 18 kHz band.

C. Similarities Between “12 kHz” and High-Frequency Anomalous Activity

Figure 10 is an excerpt from a study of the “12 kHz” phenomenon by Reynolds.¹¹ The figure shows a representative 0 to 14 kHz TOPO plot of HPFTP accel data, from E0213 static firing 904-072, which exhibits characteristic “12 kHz” activity. Historically, the “12 kHz” frequency has been shown to be very discrete and constant in frequency. A “12 kHz” amplitude of 200 Grms was observed in SSME static firing 904-028 (HPFTP u/n 2027). Typically, “12 kHz” and its related frequencies decrease in frequency at a different rate than surrounding harmonics of synchronous.¹¹ The “12 kHz” component for which the phenomenon is named is marked in the figure. Figure 11 is a TOPO plot using HPFP RAD 90 accel data from test 904-093 and is processed in identical manner to the TOPO in figure 10. Notice the similar frequency versus time behavior in the 10 to 13 kHz range of figures 10 and 11, particularly going into the slow ramp at the end of each test. Notice that the marked components do not follow the HPFTP synchronous multiple traces also marked in the TOPO’s. This is indicative of a flow-induced and/or acoustic phenomenon rather than a mechanical phenomenon driven by pump RPM.

Due to these similarities in frequency versus time behavior, the authors would denote 904-093 HPFTP data as having “12 kHz” activity. Finally, figure 12 is a 0 to 14 kHz TOPO of 904-093 high frequency pressure data from HPFP inlet (port KFIFH) processed using the same parameters as the TOPO’s of figures 10 and 11. The marked components of figure 10 are common to those of figure 11 and are a subset of the anomalous frequencies in the 10 to 18 kHz spectrum discussed previously. In other words, the anomalous frequencies from 904-093 HPFTP data which resemble “12 kHz” activity also appear in LPF duct data, and, since bicoherence did identify correlation between “330 Hz” and the 10 to 18 kHz frequencies, a correlation between “330 Hz” and “12 kHz” is implied. This implied correlation can be verified by using bicoherence techniques on high frequency data which contain “330 Hz,” definite “12 kHz,” and 10 to 18 kHz activity from the LPF duct. This verification cannot be accomplished with current test data due to loss of phase relationships among transducers due to data recording configurations.

III. CONCLUSIONS AND RECOMMENDATIONS

Edgetones modulated by the acoustic characteristics of the LPF duct and the LPFTP are implicated as the possible source of “330 Hz” and the 10 to 18 kHz band of anomalous frequencies detected in LPF duct high frequency transducers. “12 kHz” and its related frequencies which are common in HPFTP radial accel data may be a subset of the 10 to 18 kHz band of anomalous frequencies discussed in this report. Advanced spectral analysis techniques developed by Dr. Jen Jong of Wyle Laboratories have indicated a strong correlation between “330 Hz” related frequencies and the 10 to 18 kHz anomalous behavior. This, in turn, implies a global correlation between “330 Hz,” the 10 to 18 kHz anomalous behavior, and the “12 kHz” activity.

The question remains as to the detrimental effects, if any, of the higher frequencies on structural components. As shown, the energy conveyed by these higher frequencies is relatively low. However, the lack of experimental data on the high frequency modal characteristics of components such as the flex joint tripod leg make it impossible to rule out any possible resonance behavior. Experience has shown that no hardware damage has been directly related to these frequencies.

A great amount of accel, strain gauge, and high frequency pressure data has been accumulated in support of the LPF duct FJ "C" tripod leg failure investigation. Unfortunately, during the investigation, we were unable to develop key ordinary linear and higher order coherences above 5 kHz. Acquisition on independent analog recorders prevented conservation of phase among many of the LPF duct and attached turbopump transducers. With the parallel recording of several key LPFTP-LPF duct-HPFTP transducers on the same analog tape, relative phase between transducers can be retained, and these key coherences involving anomalous spectral components can be developed. There is still a considerable question and debate as to the source of these frequencies. It cannot clearly be determined which of the anomalous frequencies are causal and which are secondary. In addition, the analysis would be aided by determining the direction of propagation of these anomalies in the duct. This can only be done with an appropriately spaced array of sensors.

Emphasis should be placed on slow thrust ramps during engine tests in order to better quantify the relationship between frequencies' occurrence and flow rates. Moreover, fuel vent scheduling must be considered and its effects quantified. Hopefully, further testing will allow a mechanism to be defined and will narrow down the list of flow conditions and/or structure(s) which could be responsible for the phenomena.

Old "12 kHz" should be reexamined out to 20 kHz and compared to LPF duct data processed out to the same frequency. There exists a possibility that the new 10 to 18 kHz anomalous frequencies seen in LPF duct data have been inherent in HPFTP radial accel data for a long time.

The distinctness of these anomalous frequencies relative to engine component configuration for a given test has been noted. Efforts should continue to explore and quantify the correlations between different pump and duct combinations. Is this characteristic of certain pumps and ducts or is it more generic?

Finally, are any of these frequencies, "330 Hz," "1,300 Hz," "2,700 Hz," "12 kHz," 10 to 18 kHz, possibly detrimental to any of the components of the engine? Modal analysis of structures in the flow should be extended to 20 kHz in order to investigate these effects. Lift coefficients on components should be calculated from pressure data and compared to structural limits.

Tests could be designed and implemented on the technology test bed (TTB) facility at MSFC to systematically investigate these anomalous frequencies associated with the fuel flow system of the SSME. If a likely mechanism(s) can be defined for the anomalous frequencies listed in this report and this mechanism(s) has been determined to cause significant structural loading, the problem along with potential fixes should be verified with laboratory flow tests.

REFERENCES

1. Purmort, W.P.: "LPFTP Discharge Duct Flex Joint Tripod Failure Investigation Final Report." Rockwell International Canoga Division Internal Letter No. 1-21-028, May 23, 1991.
2. Jong, J.Y.: "Correlation Identification Between Spectral Components in Turbomachinery Measurements by Generalized Hyper-Coherence." To be Published in the proceedings of the 3rd International Machinery Monitoring and Diagnostic Conference, December 1991.
3. Jong, J.Y.: "Some Nonlinear Methods and Their Application to Rocket Engine Diagnostic Evaluation." 1st International Machinery Monitoring and Diagnostic Conference, September 1989.
4. Jong, J.Y.: "Diagnostic Assessment of Turbomachinery by the Hyper-Coherence Method." NASA Conference Publication 2436, Advanced Earth-To-Orbit Propulsion Technology, May 1986.
5. Jong, J.Y.: "A Nonlinear Coherence Function and its Application to Machine Diagnostics." 110th Meeting of the Acoustical Society of America, November 1985.
6. Shinguichi, B.: "LPFTP Low NPSP Vibration Investigation." Rockwell International Canoga Division Internal Letter No. 0170TM-757, September 16, 1980.
7. Jong, J.Y.: "Diagnostic Analysis of SSME Dynamic Data." Monthly Progress Report, NASA Contract Number NAS8-36549, February 1989.
8. Wilbanks, J.A.: "LPFP Anomalous Frequency Analysis." Rockwell International Huntsville Division Internal Letter No. 90-112-JAW-004, September 29, 1989.
9. Brown, G.B.: "The Vortex Motion Causing Edgetones." Proc. Phys. Soc., vol. 49 (1937), p. 493.
10. Wood, A.: "Acoustics." Dover Publications, New York N.Y., 1966, pg. 403.
11. Reynolds, T.R.: "HPFTP '12 kHz' Anomalous Frequency Analysis." Rockwell International Huntsville Division, August 27, 1990.

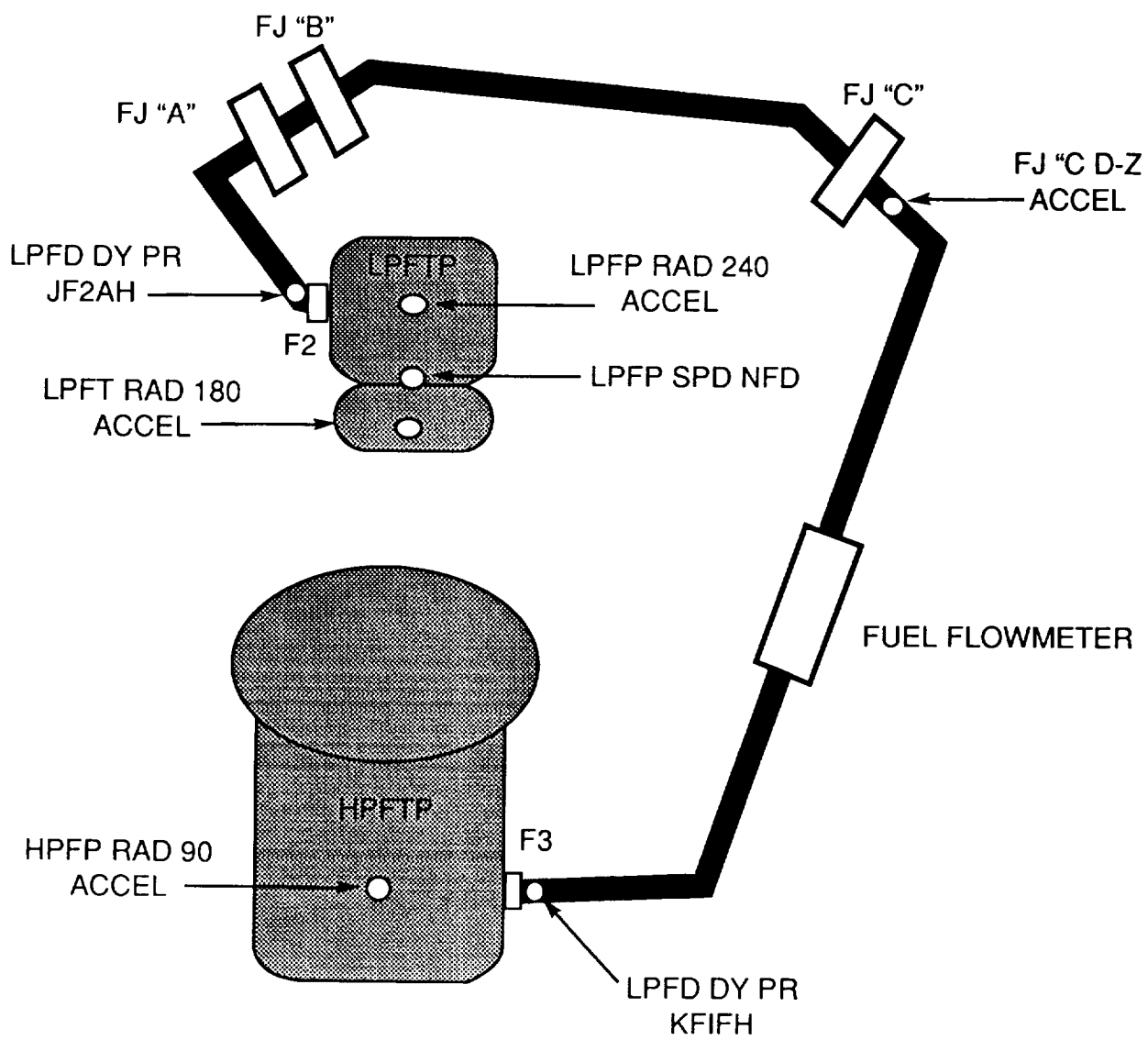


Figure 1. Transducer location.

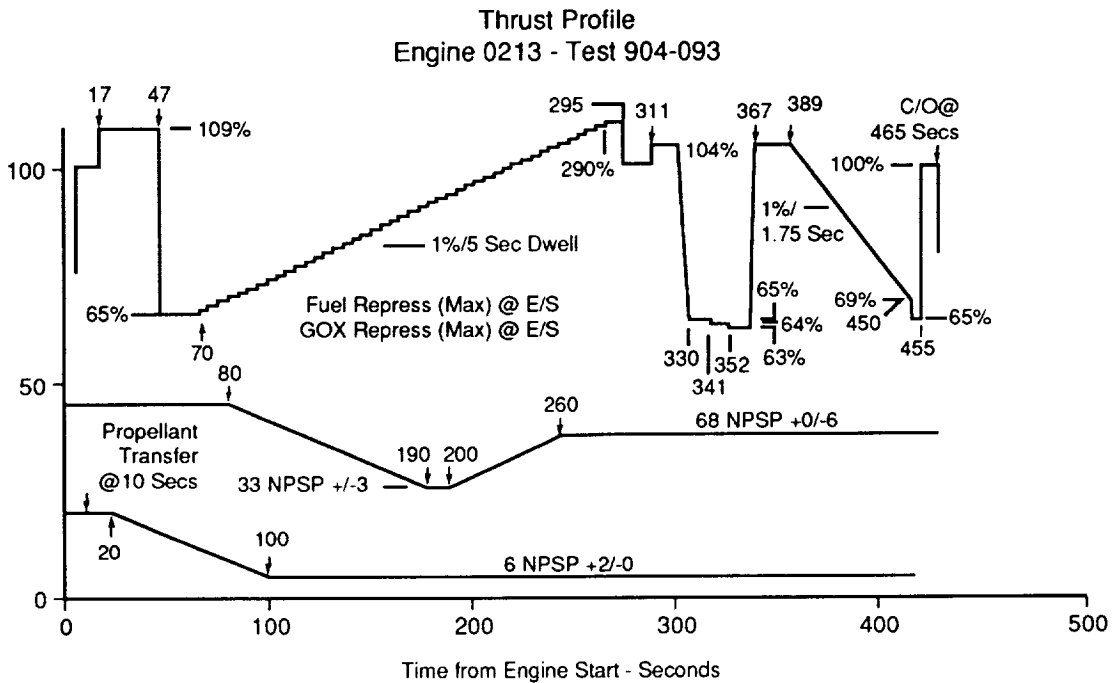
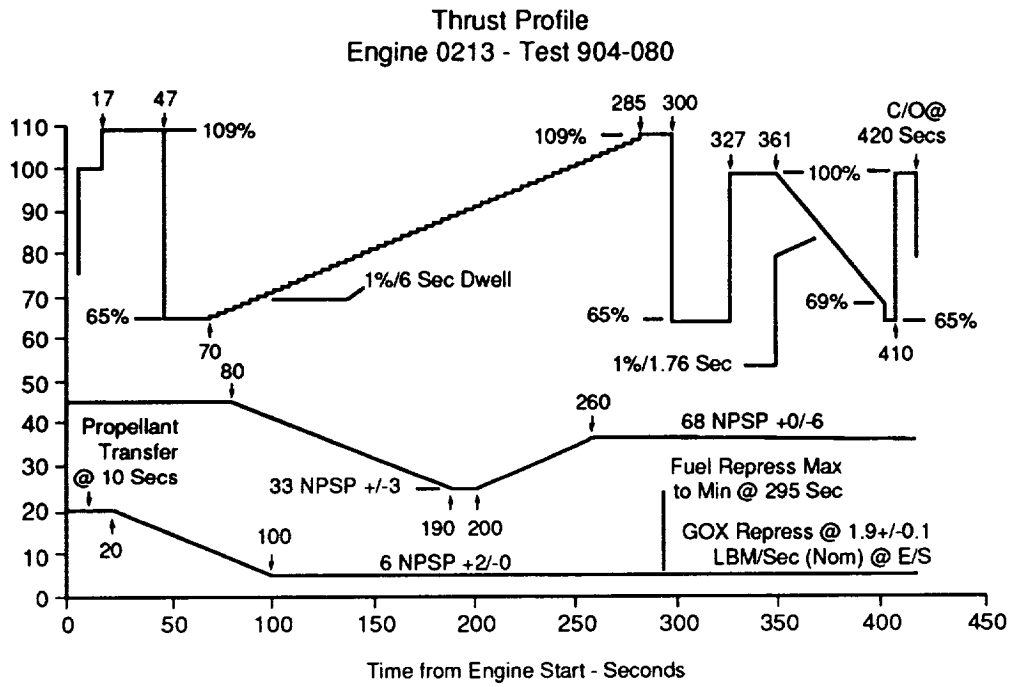


Figure 2. 904-080 and 904-093 thrust profiles.

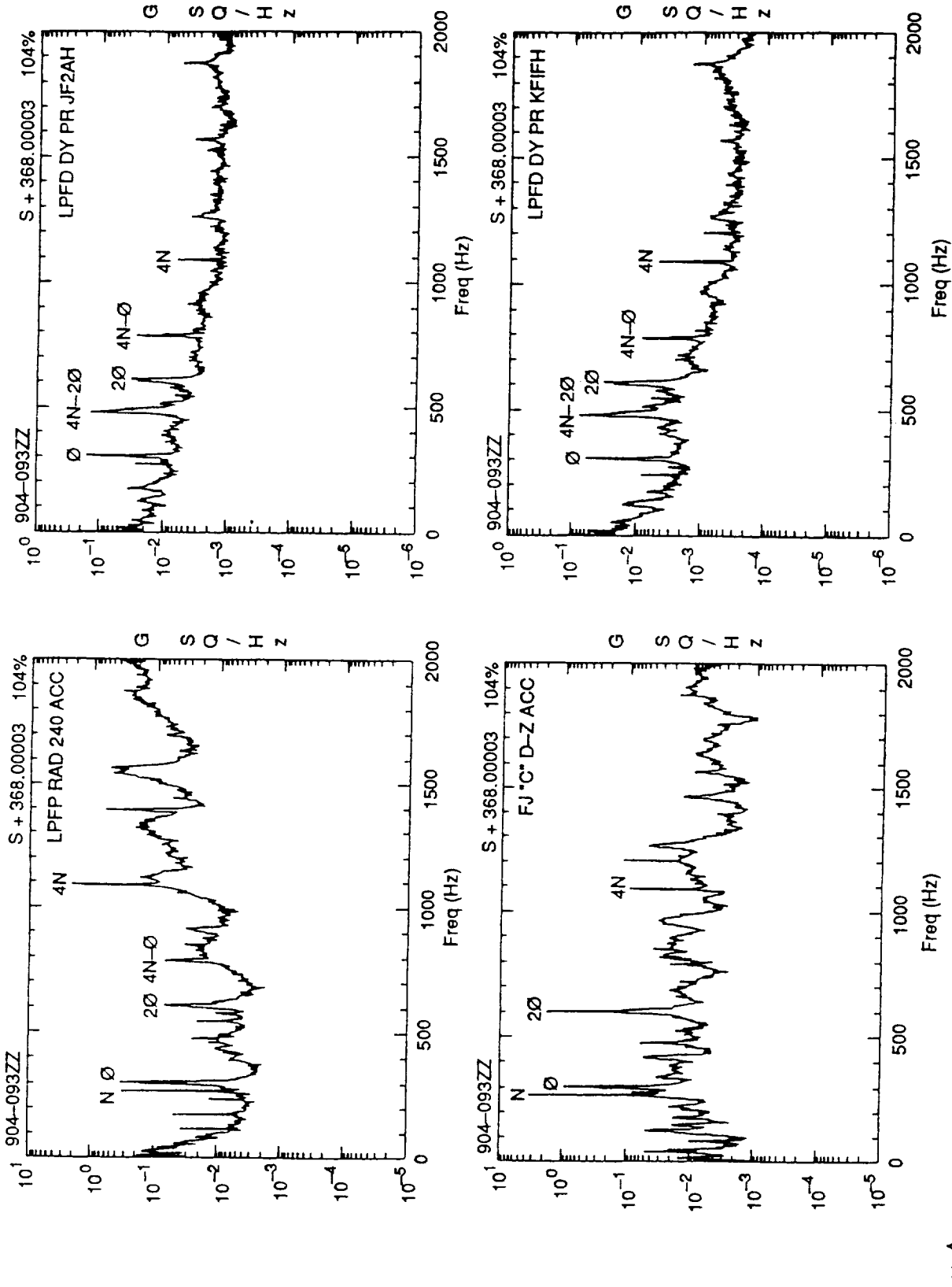
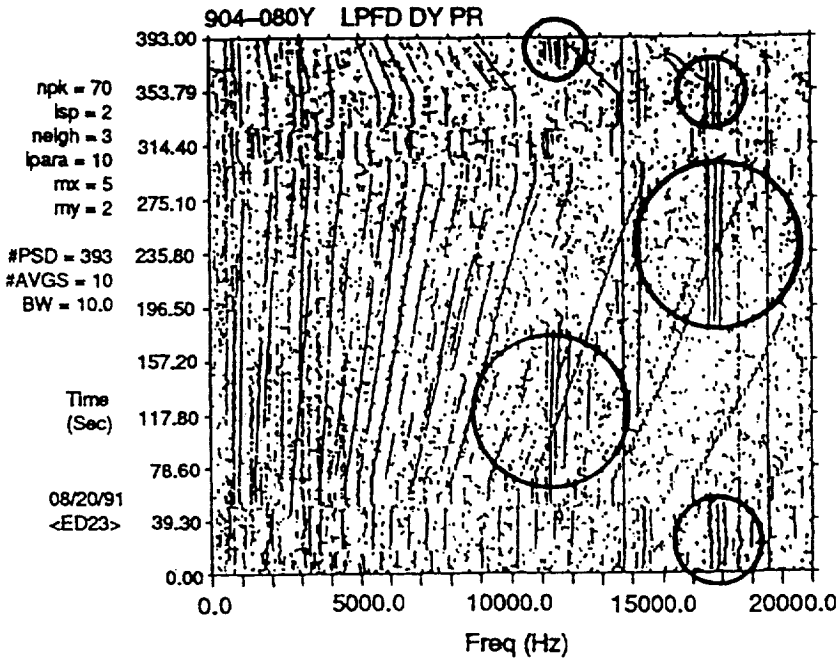
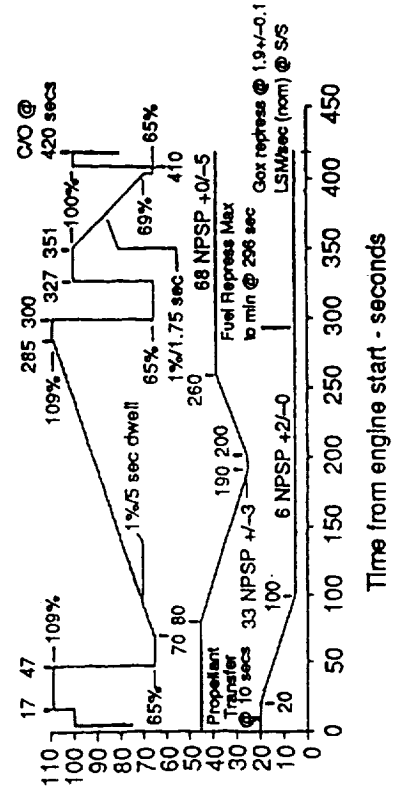


Figure 3. PSD's showing "330-Hz" activity, SSME static firing 904-093.



Thrust Profile
Engine 0213 - Test 904-080



Thrust Profile
Engine 0213 - Test 904-093

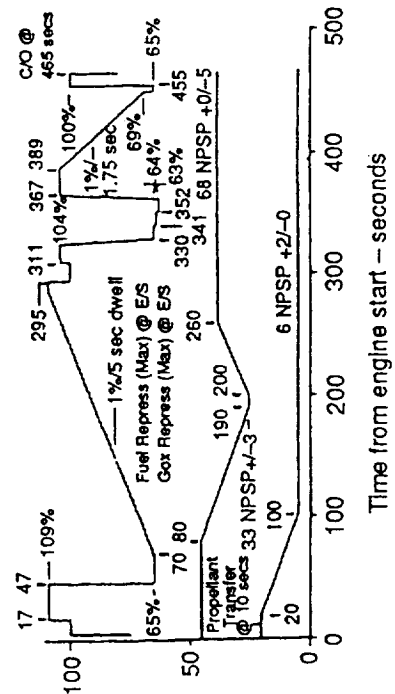


Figure 4. TOPO plots of LPF duct dynamic pressure for tests 904-080 and 904-093.

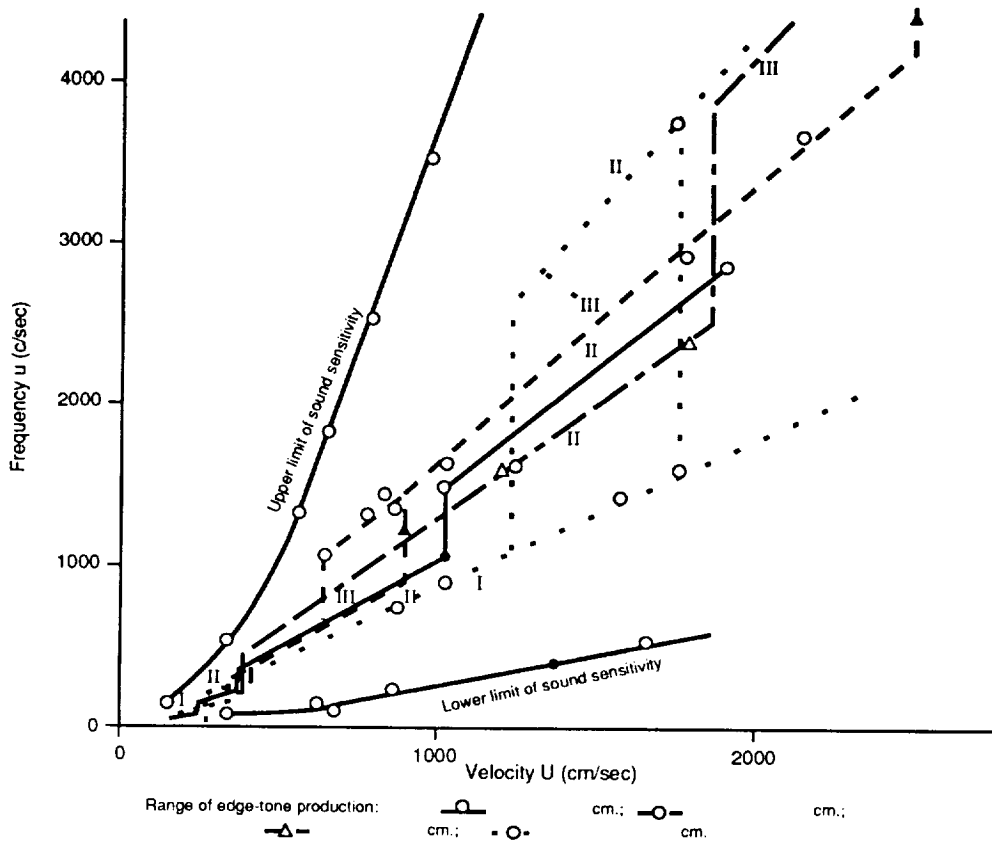


Figure 5a.

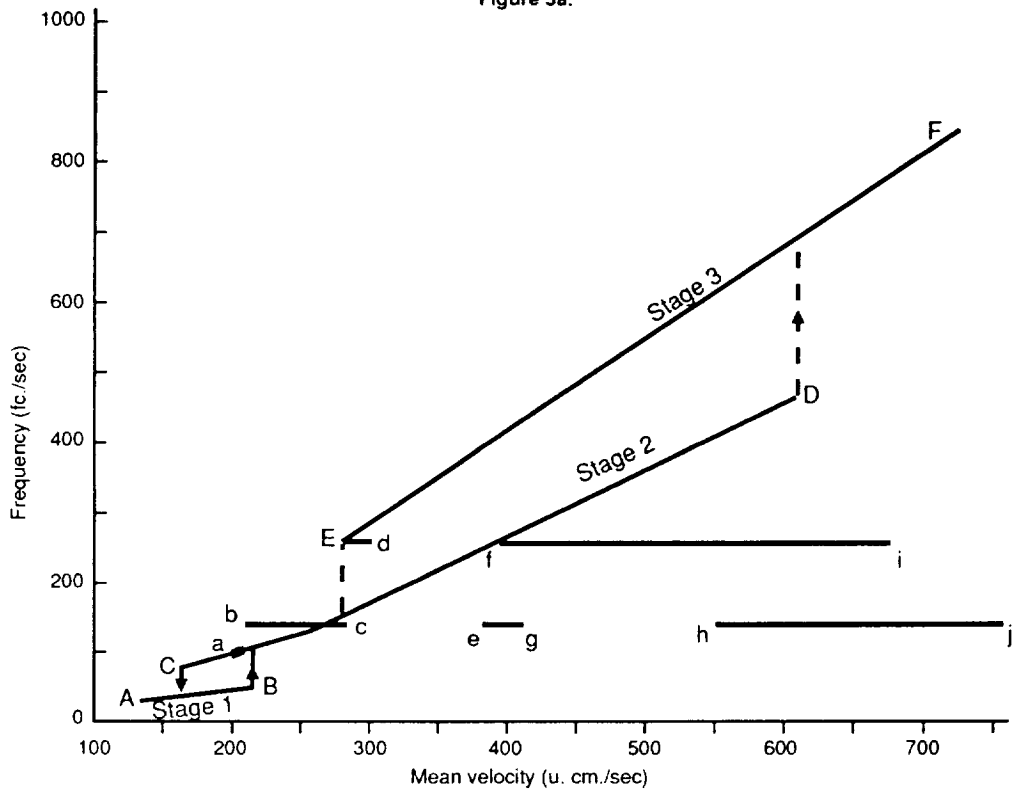
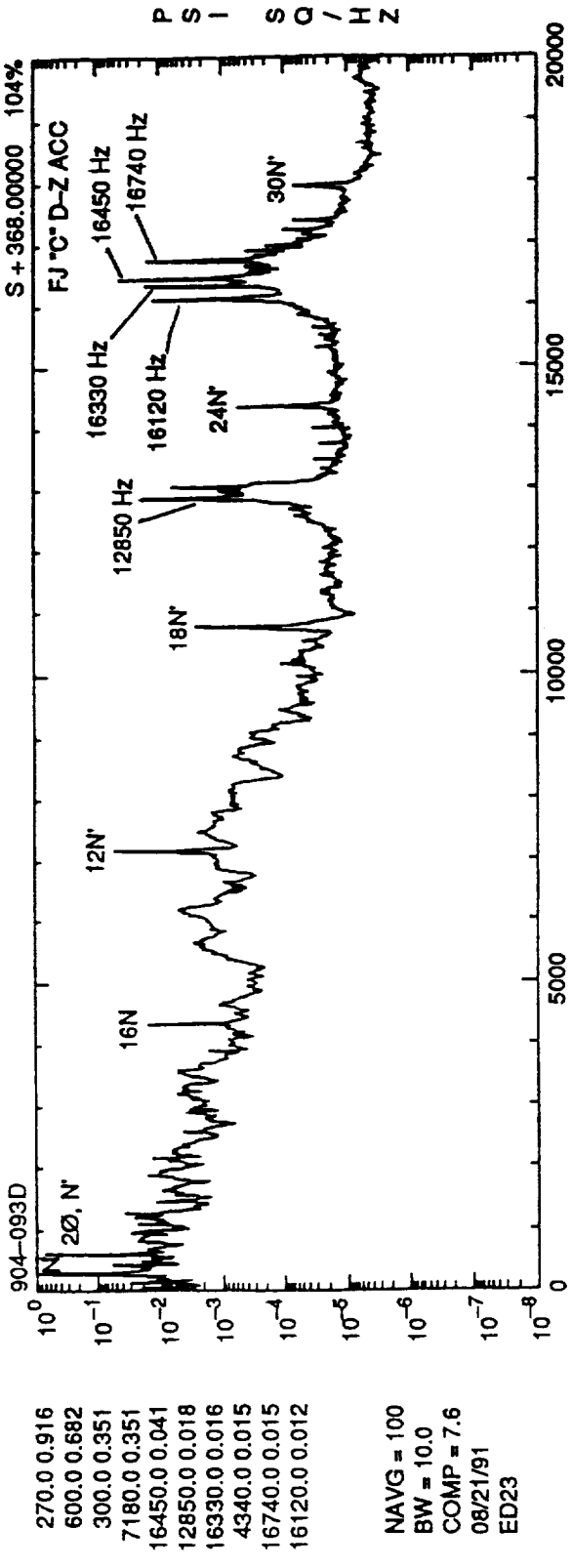


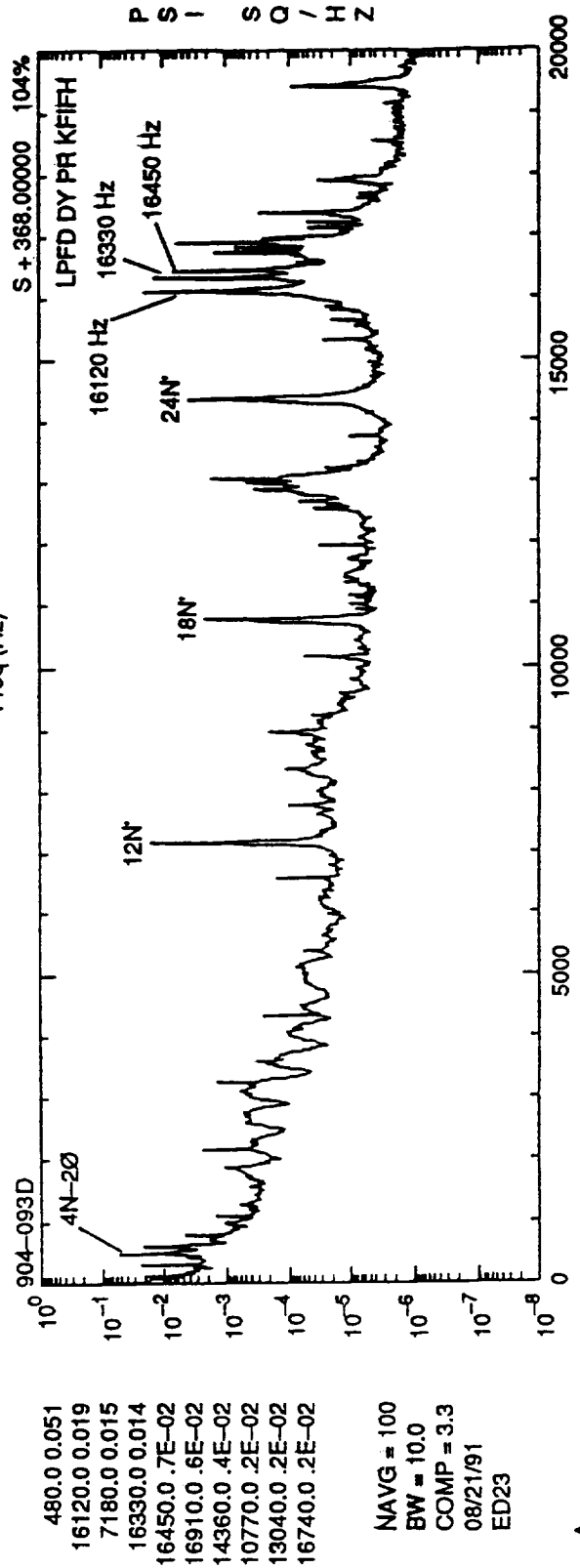
Figure 5b.

Figure 5. Experimental edgetone acoustics.



270.0 0.916
 600.0 0.682
 300.0 0.351
 7180.0 0.351
 16450.0 0.041
 12850.0 0.018
 16330.0 0.016
 4340.0 0.015
 16740.0 0.015
 16120.0 0.012

NAVIG = 100
 BW = 10.0
 COMP = 7.6
 08/21/91
 ED23



480.0 0.051
 16120.0 0.019
 7180.0 0.015
 16330.0 0.014
 16450.0 .7E-02
 16910.0 .6E-02
 14360.0 .4E-02
 10770.0 .2E-02
 13040.0 .2E-02
 16740.0 .2E-02

NAVIG = 100
 BW = 10.0
 COMP = 3.3
 08/21/91
 ED23

N Δ LPFTP Synchronous
 N' Δ HPFTP Synchronous
 Ø Δ "330 Hz"

Figure 6. PSD's of LPFD duct DY PR KFIFH and FJ "C" D-Z accel.

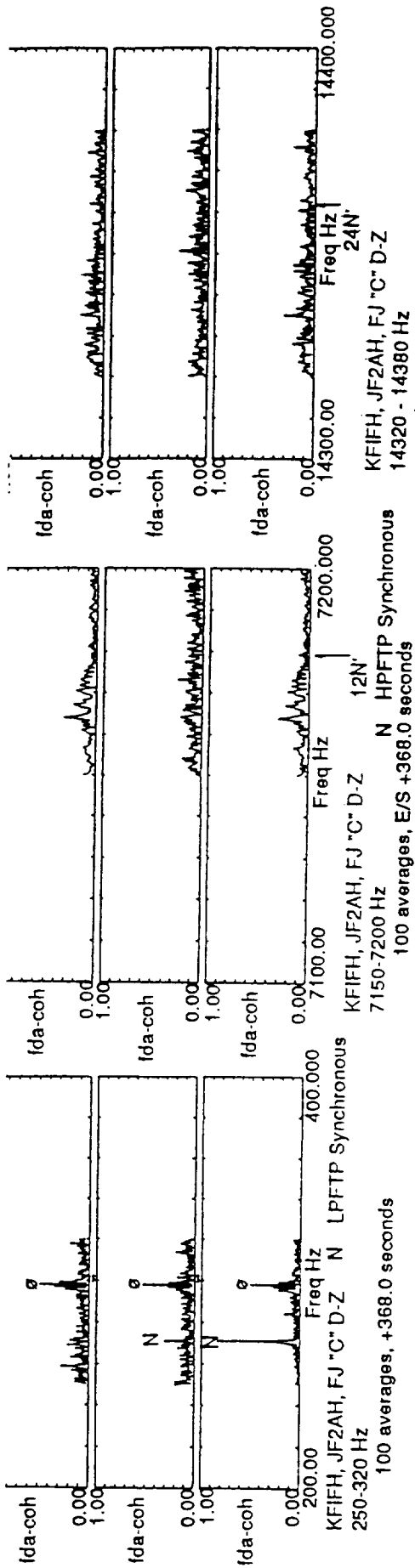


Figure 7a. PDA Coherence for LPFTP Sync (N) and "330 Hz" Figure 7b. PDA Coherence for 12N'

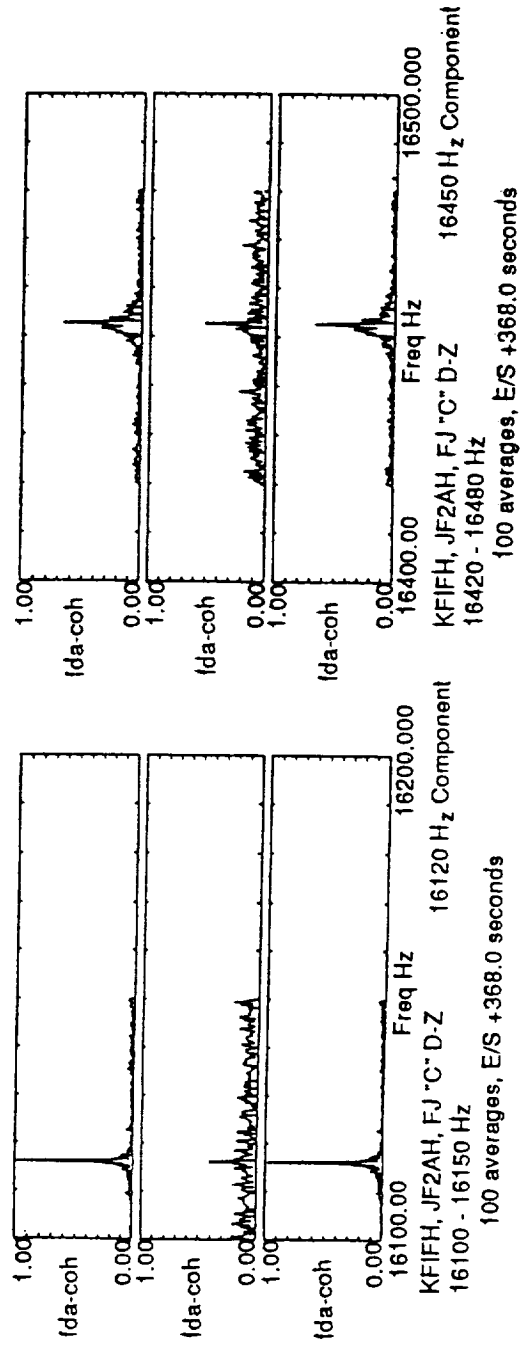


Figure 7b. PDA Coherence for 16,120 Hz Anomalous Component Figure 7c. PDA Coherence for 24N'



Figure 7c. PDA Coherence for 24N' Figure 7d. PDA Coherence for 16,120 Hz Anomalous Component Figure 7e. PDA Coherence for 16,450 Hz Anomalous Component



Figure 7d. PDA Coherence for 16,120 Hz Anomalous Component Figure 7e. PDA Coherence for 16,450 Hz Anomalous Component



Figure 7e. PDA Coherence for 16,450 Hz Anomalous Component

Figure 7. PDA coherence plots.

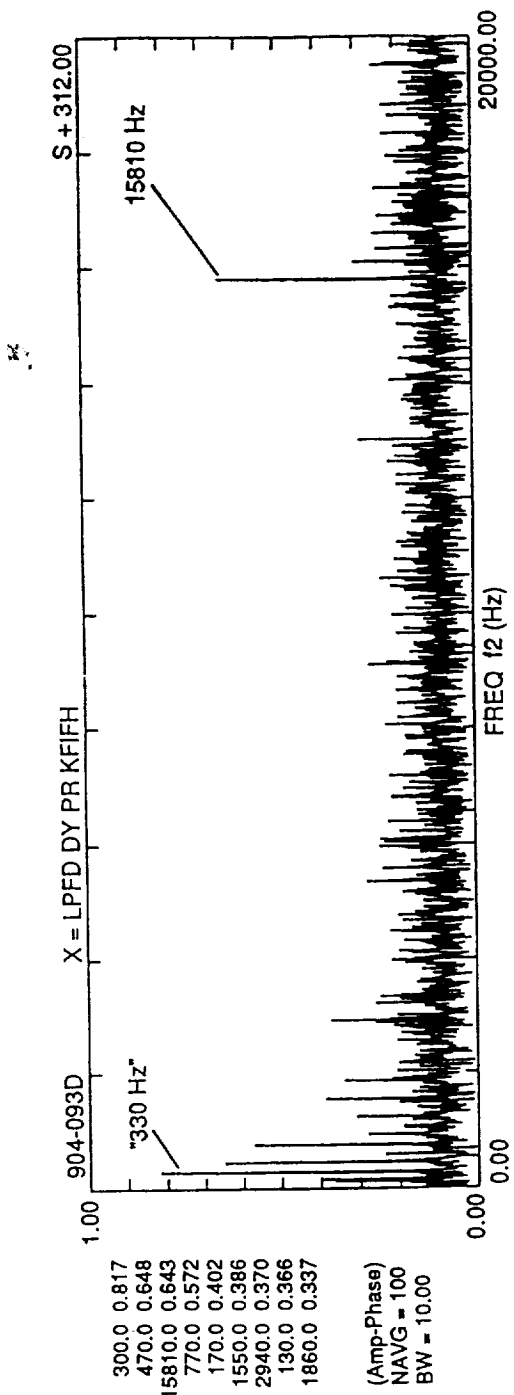


Figure 8. Bicoherence plot HPFTP inlet at KFIFH.

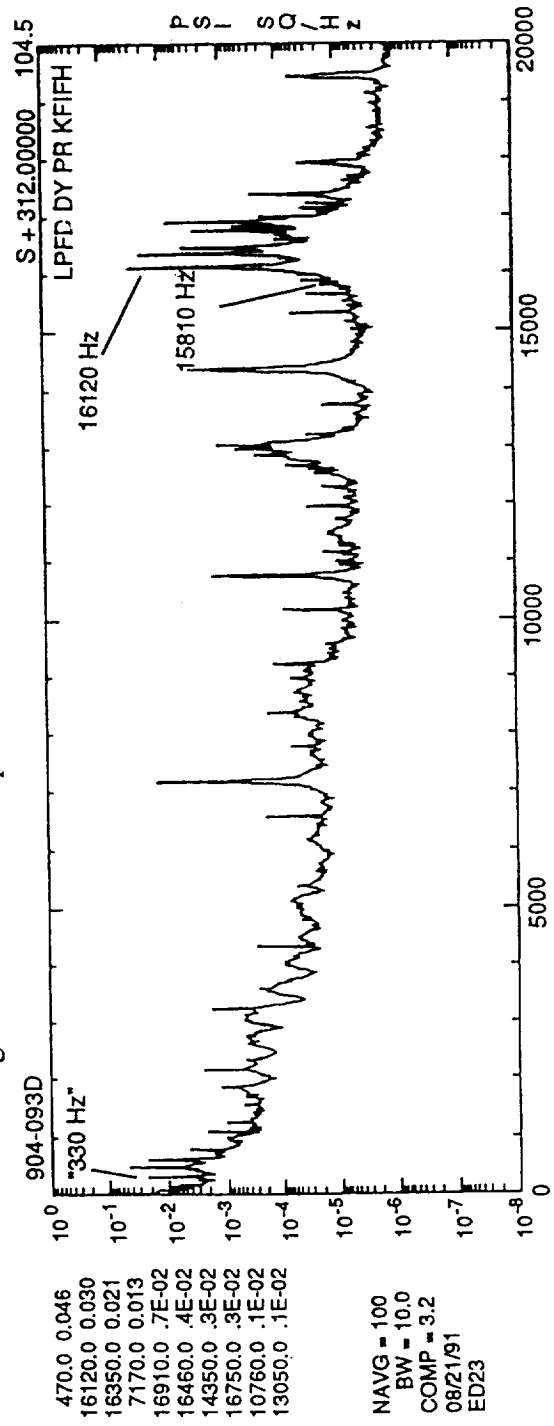


Figure 9. Corresponding PSD for bicoherence plot of figure 8.

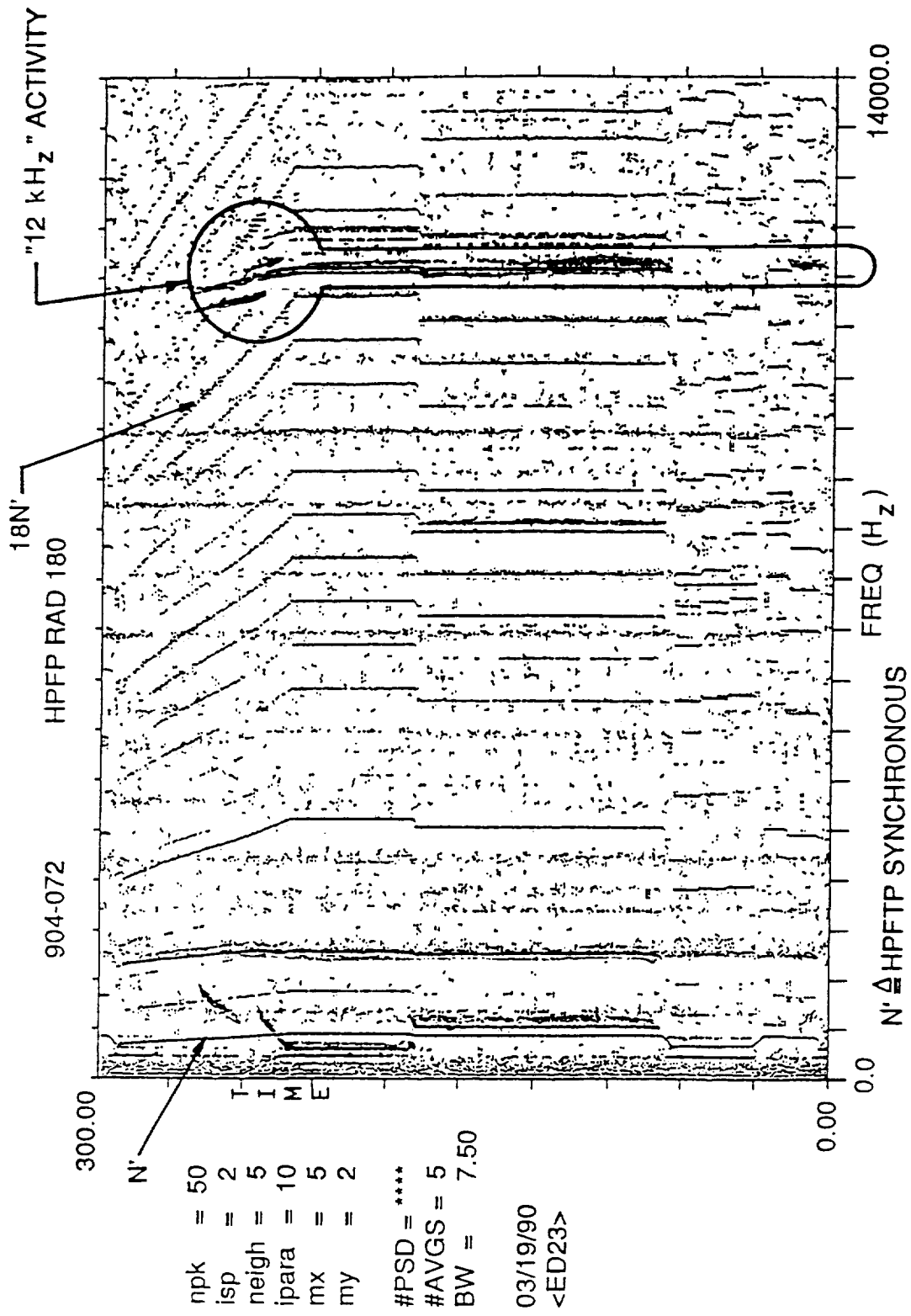


Figure 10. TOPO of 904-072 HPFTP radial accel data.

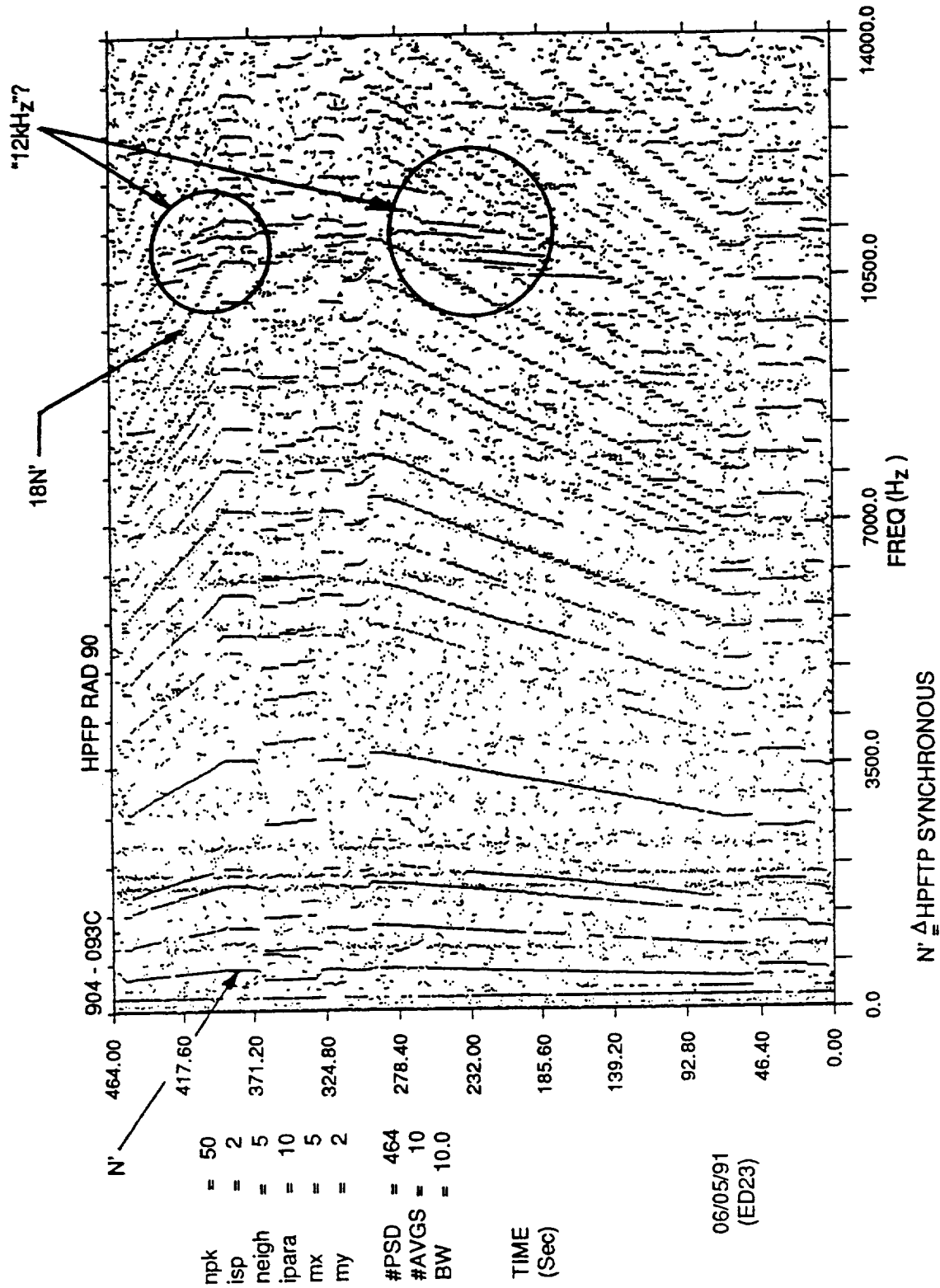


Figure 11. TOPO of 904-093 HPFTP radial accel data.

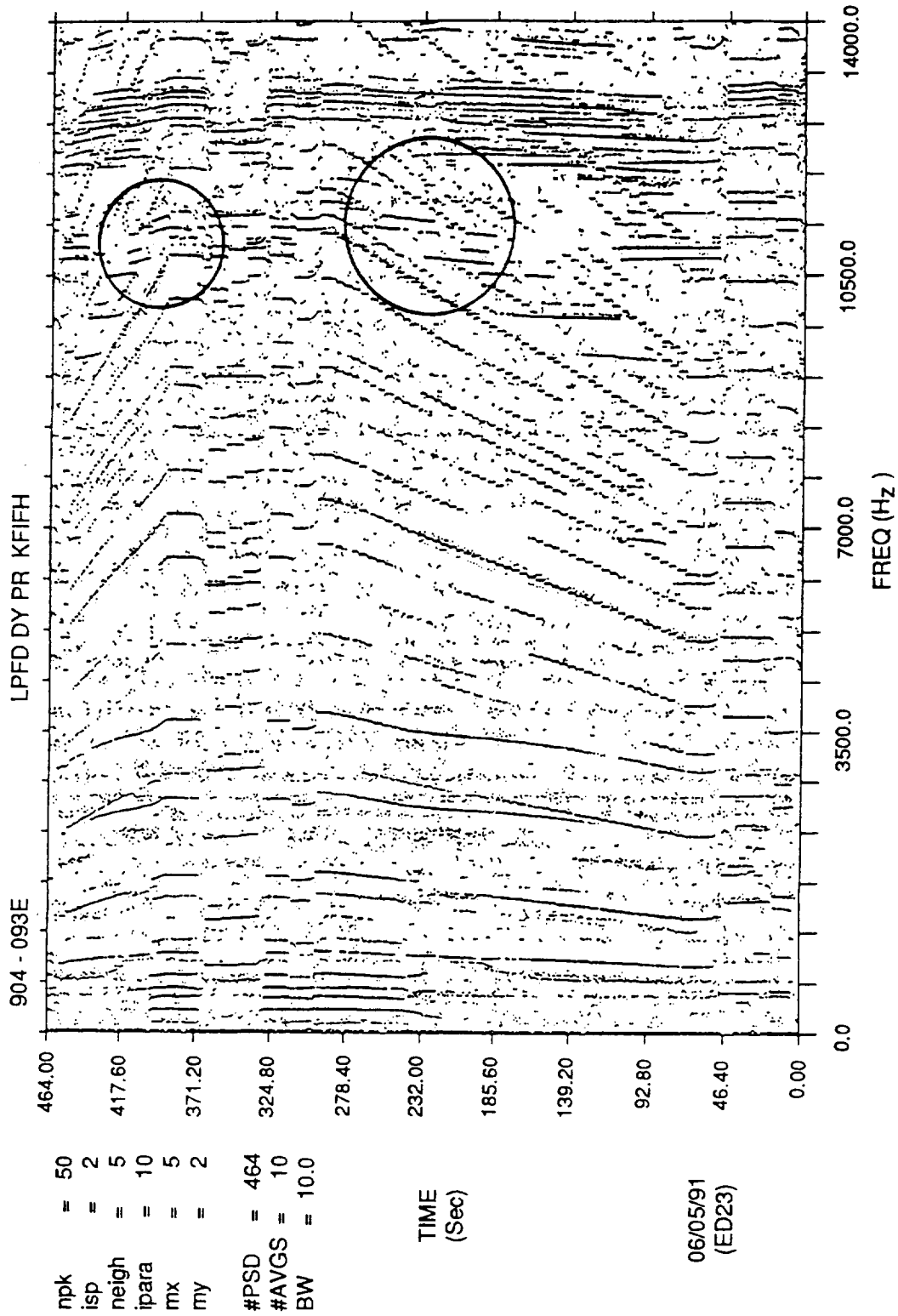


Figure 12. TOPO of 904-093 HPFP high-frequency inlet pressure at KFIH.

APPROVAL

**HIGH-FREQUENCY DATA OBSERVATIONS FROM
SPACE SHUTTLE MAIN ENGINE LOW PRESSURE FUEL TURBOPUMP
DISCHARGE DUCT FLEX JOINT TRIPOD FAILURE INVESTIGATION**

By T.F. Zoladz and R.A. Farr

The information in this report has been reviewed for technical content. Review of any information concerning Department of Defense or nuclear energy activities or programs has been made by the MSFC Security Classification Officer. This report, in its entirety, has been determined to be unclassified.



J.C. BLAIR

Director, Structures and Dynamics Laboratory